A Comparative Analysis of Fourier Transform, Wavelet Transform and Empirical Mode Decomposition in Denoising Photoplethysmographic Signal Towards Stress Detection

A thesis

Submitted in partial fulfillment of the requirements for the Degree of

Bachelor of Science in Computer Science and Engineering

Submitted by

Tahlamuna Rulpi	**170204083**
Jesmin Akhter	**180104052**
Ramisa Maliyat	**180104079**
Sadia Sultana	**180104094**

Supervised by

Md. Aminur Rahman

Department of Computer Science and Engineering

Ahsanullah University of Science and Technology

Dhaka, Bangladesh

December 2022

CANDIDATES' DECLARATION

We, hereby, declare that the thesis presented in this report is the outcome of the investigation performed by us under the supervision of Md. Aminur Rahman, Department of Computer Science and Engineering, Ahsanullah University of Science and Technology, Dhaka, Bangladesh. The work was spread over two final year courses, CSE4100: Project and Thesis I and CSE4250: Project and Thesis II, in accordance with the course curriculum of the Department for the Bachelor of Science in Computer Science and Engineering program.

It is also declared that neither this thesis nor any part of has been submitted anywhere else for the award of any degree, diploma or other qualifications.

Tahlamuna Rulpi
170204083

Jesmin Akhter
180104052

Ramisa Maliyat
180104079

Sadia Sultana
180104094

CERTIFICATION

This thesis titled, **"A Comparative Analysis of Fourier Transform, Wavelet Transform and Empirical Mode Decomposition in Denoising Photoplethysmographic Signal Towards Stress Detection"**, submitted by the group as mentioned below has been accepted as satisfactory in partial fulfillment of the requirements for the degree B.Sc. in Computer Science and Engineering in December 2022.

Group Members:

Tahlamuna Rulpi	**170204083**
Jesmin Akhter	**180104052**
Ramisa Maliyat	**180104079**
Sadia Sultana	**180104094**

Md. Aminur Rahman
Assistant Professor & Supervisor
Department of Computer Science and Engineering
Ahsanullah University of Science and Technology

Prof. Dr. Md. Shahriar Mahbub
Professor & Head
Department of Computer Science and Engineering
Ahsanullah University of Science and Technology

ACKNOWLEDGEMENT

First and foremost, we would like to express our gratitude to the Almighty ALLAH for successful completion of our thesis work. We would like to take this convenience to thank AHSANULLAH UNIVERSITY OF SCIENCE AND TECHNOLOGY for providing us with such a graceful opportunity to become part of this institution. It has been a privilege for us to pursue the Degree of Bachelor Science In Computer Science And Engineering here.

We would like to express our heartiest gratitude and sincere appreciation to our honourable thesis supervisor Md. Aminur Rahman, Assistant Professor, Department of Computer Science and Engineering, AUST. Without his timely advices, continuous guidance and supervision, all these works would not have been possible at all.

We would like to thank all the persons that are related to our thesis work directly and indirectly.

Dhaka
December 2022

Tahlamuna Rulpi

Jesmin Akhter

Ramisa Maliyat

Sadia Sultana

ABSTRACT

Major global concerns now include stress and mental health. Numerous psychophysiological illnesses may be implicated by persistent stress. The chance of depression, stroke, heart attack, and cardiac arrest, for instance, increases with stress. The field's emphasis has evolved in recent years from the laboratory to the actual world. To assess stress, signals can be gathered through wearable technology. The chest, head, wrist, and other places can all accommodate these devices. It makes daily living easier and more convenient if sensors are linked to the wrist. However, several internal and external sounds can interfere with these signals. Signals for ubiquitous and real-time measuring systems are very highly susceptible to motion artifacts (MA), which could produce unreliable results. So,one of the major steps of stress detection is to denoise the signal. Wearable Stress and Affect Detection Dataset is the public dataset that we have used (WESAD). Photoplethysmogram (PPG) data were obtained from this dataset. The purpose of our work is to compare three signal decomposition methods- Fourier transform, Wavelet transform, and Empirical Mode Decomposition(EMD) to remove the various noises present in the PPG signals and extract the features of interest for accurate detection of stress and monitoring of people's health status. Considering the binary classification(stress vs non-stress) problem we achieved classification accuracies of up to 99%. Among the three methods wavelet transform has the best performance.

Keywords: Stress, Physiological signals, Wearable devices, Photoplethysmogram, Fourier transform, Wavelet transform,Empirical Mode Decomposition(EMD).

Contents

List of Figures

List of Tables

Chapter 1

Introduction

1.1 Introduction

Any kind of change that puts physical, mental, or psychological strain on a person is considered to be stressful. Body's reaction to anything that demands focus or action is stress. Everyone goes through periods of stress. Knowing one's stress level with accuracy has become crucial. Chronic stress is extremely harmful to both physical and psychological health since it causes cancer, cardiovascular disease, depression, and diabetes. Self-report assessments, behavioral coding, or physiological measurements can all be used to assess stress responses. These reactions to stressful events include feelings, thoughts, behaviors, and physiological reactions. It is crucial to develop reliable techniques for the quick and precise identification of human stress. In the past, questionnaires were used to measure levels of stress. Wearable sensors are now utilized to measure physiological signals that are used to detect stress. Signals from photoplethysmograms (PPGs) and electrocardiograms (ECGs) are routinely utilized to identify stress. PPG signals are used to measure the body's blood flow and identify variations in blood volume in the peripheral circulation. Without doing any harm, it measures variations in blood circulation by employing a light source and a photodetector at the skin's surface. PPG data is gathered via sensors attached to wrist-mounted devices. Gadgets are becoming more practical, affordable, and convenient as a result. Unwanted electrical or electromagnetic energy, or noise, lowers the signal and data quality. The receiver finds it unpleasant when an unwanted signal joins a communication while it is being received. All forms of data and communications, including text, programs, photos, audio, and telemetry, can be affected by noise, which occurs in both digital and analog systems. Noise can have a great impact on performance by altering how information is processed or by changing how a person responds strategically. It specifically raises the amount of attentiveness, activation, and attention. That's why, we have to denoise the signal to get the exact performance in stress detection. Denoising is the process of isolating the

original signal from a noisy or damaged signal, and it can be applied to any signal. Taking the forward double-density DWT over four scales is the initial step in denoising the signal. The wavelet coefficients are then subjected to a denoising technique called soft thresholding over all scales and subbands. Denoising methods are applied in terms of frequency and duration. In our study, we have used the Fourier transform, Wavelet transform, and Empirical Mode Decomposition(EMD) as denoising techniques and compared the performance of the noisy signal and denoised signal. In Fourier transform, we used an ensemble-based peak identification technique. In order to construct wavelets, the input from each sensor was split into six distinct signals using a sliding window. The fundamental premise of wavelet thresholding, also known as wavelet denoising, is that many real-world signals result in a sparse representation thanks to the wavelet transform. Ten statistical features were then extracted from the denoised signals using BioSPPy. We used the mother wavelets haar, db4, and sym8 to denoise these signals using soft thresholding and the BayesShrink method. Each IMF is filtered or thresholded as part of the EMD denoising process, which then uses the processed IMFs to reconstitute the estimated signal. The EMD can be used in conjunction with nonlinear transformation or a filtering strategy. A signal is divided into components known as intrinsic mode functions(IMFs) by the process of empirical mode decomposition (EMD). Ten statistical features were extracted using BioSPPy from the IMF component and residue after denoising the appropriate IMF component and residue for feature extraction.

1.2 Motivation

Stress is a word we use frequently in our daily lives. We may experience stress when we have several obligations that we are finding difficult to handle. Acute stress, which occurs within a few minutes to a few hours following an occurrence, is often helpful in completing activities and making us feel more energized. However, chronic stress, which is stress that keeps returning, is stress that lasts for a long period or is highly intense. Our physical and mental health may be impacted by stress in specific situations. And it can worse issues that are already present. Recognizing typical stress symptoms might aid in managing them. Chronic stress can be a factor in a number of health issues, including high blood pressure, breathing difficulties, heart disease, obesity, and diabetes. We were encouraged to work on this topic since these pressing challenges may encourage individuals to take good care of their health before unfavorable things occur. Doing the right actions at the right moment, also assists people in overcoming stress. PPG devices are currently commonly utilized since they are practical, inexpensive, low-powered, and manageable owing to their tiny size. We decide to handle this signal as a result.

1.3 Objective

Our research aims to enhance stress detection performance. Wearable gadgets like wrist, head, or chest devices, among others, can gather signals for stress detection. This signal performs better when used after the noise has been reduced than when used without any noise reduction. In this investigation, we will examine whether technique—Fourier transform, Empirical Mode Decomposition, or wavelet transform—performs best on PPG signals to minimize noise. The data are gathered by attaching sensors to the wrist, and PPG is a signal that depicts a shifting arterial wave throughout each cardiac cycle. As a result, setting up devices is simple and affordable. In this study, we employed a publicly available dataset (WESAD) that has a wealth of relevant data and offers a variety of physiological signals that are labeled with three emotional states: baseline, stress, and amusement.

1.4 Thesis Organization

In our research, our main aim is to see which denoising method performs better to reduce noise from PPG signals.

Chapter 1 (Introduction): In this chapter, we have discussed problem definition, basic concepts and our aim to use Machine learning (ML) to detect stress.

Chapter 2 (Literature Review): In this chapter, we have discussed a short description of related papers which we have studied. We have also explained our transformation techniques here.

Chapter 3 (Methodology): In this chapter, we have discussed our techniques for denoising PPG signals to detect stress, and peak detection methods. We have also explained our work ideas and features. We have discussed the WESAD dataset here.

Chapter 4 (Experimental Result): In this chapter, we have discussed our experimental setup and results.

Chapter 5 (Conclusion And Future work): Here we have finished up our paper by featuring our topic. Probable future plans and ideas are also described here.

Chapter 2

Literature Review

2.1 Denoising Techniques in Signal Processing

2.1.1 Fourier Transformation

The Fourier transformation is a mathematical formula that relates a signal sampled in time or space to a similar signal sampled in frequency. It is a translation between two mathematical worlds: signals and frequency.

Cycle-by-cycle from PPG data tainted by motion distortions, clean PPG is extracted using Fourier series analysis. [6]

Let, f(t) represent the periodic signal with the T period. Fourier series will be,
$f(t) = a_0 + \sum_{k=1}^{\infty} a_k cos(kwt) + b_k sin(kwt)$ .....(1) $Where$
$w = \frac{2\pi}{T}$ .....(2)
$a_0 = \frac{1}{T}\int_0^T f(t)t$ ..... (3)
$a_k = \frac{2}{T}\int_0^T f(t)cos(kwt)dt$ ..... (4)
$b_k = \frac{2}{T}\int_0^T f(t)sin(kwt)dt$ ..... (5) [6]
Fourier transformation cannot be directly applied to a PPG signal. By applying the cycle-by-cycle Fourier series the problem is solved. Now,

$$f_c(t) = f(t) + f_a(t)$$

Where $f_c(t)$ represents the resultant corrupted PPG signal and

f(t) is the original artifact-free PPG signal

$f_a(t)$ is the motion artifact.

Compute the Fourier series coefficients of the m^{th} cycle, we get,

$$\begin{aligned} \mathrm{ma}_{0c} &= \frac{1}{Tm}\int_0^{Tm} f_c(t)dt \\ &= \frac{1}{Tm}\int_0^{Tm}[f(t)+f_a(t)]dt \\ &= \mathrm{m}^{a_0} + \frac{1}{Tm}\int_0^{Tm} f_a(t)dt \quad \ldots\ldots\ldots (8) \end{aligned}$$

$$\mathrm{m}^{a_{kc}} = m^{a_k} + \frac{2}{Tm}\int_0^{Tm} f_a(t)cos(kw_m t)dt \quad \ldots\ldots\ldots (9)$$

$$\mathrm{m}^{b_{kc}} = m^{b_k} + \frac{2}{Tm}\int_0^{Tm} f_a(t)sin(kw_m t)dt \quad \ldots\ldots\ldots (10)$$

Here,

$\frac{1}{Tm}\int_0^{Tm} f_a(t)cos(kw_m t)dt$ and $\frac{1}{Tm}\int_0^{Tm} f_a(t)sin(kw_m t)dt$ individually would evaluate to zero, which means PPG is not correlated with motion artifacts. Applying this condition, we get,

$\mathrm{m}^{a_{kc}} = m^{a_k}$ *and*

$m^{b_{kc}} = m^{b_k}$

Here, we see that in case we reconstruct the PPG signal from the Fourier series coefficients of the corrupted PPG, the initial PPG signal can be found.

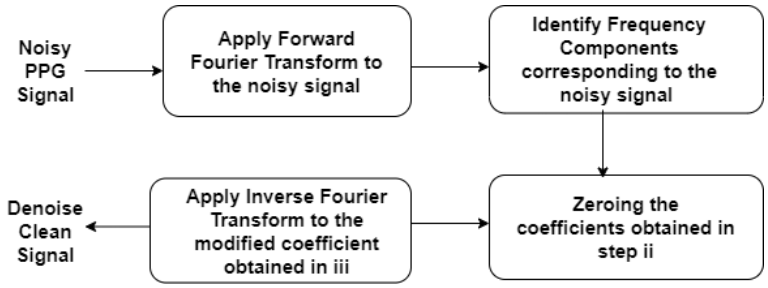

Figure 2.1: Fourier transform block diagram for signal denoising [12]

Fourier transform (FT) is used to analyze the behavior of PPG signals in the frequency domain. The signal is first transformed into the frequency domain by a fast Fourier transform (FFT). After being transformed, the basic frequency of the PPG signal is used to detect peak values. The signal is reconstructed by an inverse Fourier transform taking first and second harmonics. [13]

The Discrete Fourier Transformation (DFT) is implemented using the Fast Fourier transform(FFT), which is an optimized algorithm. FFT calculates the DFT as well as its inverse. The FFT technique is used to transform a digital signal (x) of length (N) from the time domain into a signal in the frequency domain (X) since the amplitude of vibration is measured as a function of the signal's evolution over frequency.

A manufactured noise reference signal will be created utilizing the Fourier transform which can be utilized as another input to the adaptive filter and will possibly dispose of the extra sensor for acquisition.

2.1.2 Wavelet Transformation

Wavelet transformations work in both the time and frequency domains simultaneously. In general, in pure periodic signals, the period is constant irrespective of time. So, in analyzing the quasi-periodic signals the Fourier transform is not adequate. Wavelet transformation provides a viable solution because they are useful for examining aperiodic, noisy signals. [12]

The unique features of wavelets distinguish wavelet signal processing from conventional signal processing approaches. Wavelet signal processing enables signal analysis at various resolutions, captures the transitory properties of signals, and can represent signals sparsely.

The Fourier transform has the significant drawback of capturing global frequency information, or frequencies that are present throughout the entire signal. It's possible that not all applications benefit from this type of signal decomposition. The wavelet transform is an alternate method that breaks down a function into a collection of wavelets. The advantage of wavelet transformation over Fourier transformation is it can capture both frequencies and location information. Wavelet transformations enable the analysis of a non-stationary signal's components. The Fourier transform is founded on a single function $\Psi(n)$ that has been scaled. However, we can shift the function in the case of the wavelet transform to produce a family of functions with two parameters $\Psi_{a,b}(n)$.

A discrete form of wavelet transformation provides adequate information and a considerable reduction in the computation time is also achieved.

Wavelet transformation for a discrete signal x (t) is defined as:

$$\text{W(p,q)} = \text{C(a,b)} = \sum_{n\epsilon Z} x(n)\Psi_{a,b}(n)$$

Where,

$$\Psi_{a,b}(n) = 2^{\frac{-a}{2}}\ \text{(n)}\ \Psi(2^{-a}n - b)$$
$$\text{p} = 2^a$$
$$\text{q} = 2^a b$$

[21]

A discrete wavelet transform(DWT) is any wavelet change for which the wavelets are translated in discrete steps.

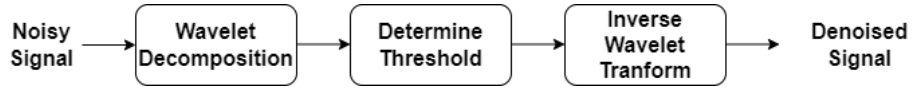

Figure 2.2: Block representation for the discrete wavelet decomposition (DWT) [31]

The PPG signal noise reduction calculations based on DWT comprise the following steps: [32]

At first, differentiate noisy signal x (t) to obtain $x_d(t)$ followed by:

$$\mathrm{x}_d(t) = (\tfrac{dx(t)}{dt})$$

At that point take the DWT of the information $x_d(t)$ and get wavelet coefficients $W_{j,k}$

Where, j refers to a scale of magnitude 2^k.

This transformation is the discrete to the analog of continuous wavelet is followed by:

$$\mathrm{W}_{j,k} = \int_{-\infty}^{+\infty} x_d(t)\Psi_{j,k}(t)dt$$

Where,

$$\Psi_{j,k}(t) = 2^{j/2}c(2^j t - k) \text{ where j,k are integers.}$$

Now, There are two forms of thresholding: hard and soft that are used to denoise any signal.

Hard thresholding is the process of reducing the coefficients whose absolute values are less than the threshold value to zero. For a given wavelet coefficient d value and threshold the definition of a hard threshold is:

$$\mathrm{D}^H(\mathrm{d}\,|\,\lambda) = 0, \quad \text{for} \quad |d| \leq \lambda$$

$$\mathrm{d}, \text{ for } \quad |d| > \lambda \qquad [34]$$

Another technique is called soft thresholding, which works by first setting all coefficients with absolute values below the threshold to zero and then reducing the absolute values of the nonzero coefficients until they are zero.

Using the following equation, soft thresholding is represented by :

$$\mathrm{D}^S(d|\lambda) = 0, \quad \text{for} \quad |\mathrm{d}| \leq \lambda$$

$$d - \lambda, \quad \text{for} \quad d > \lambda$$

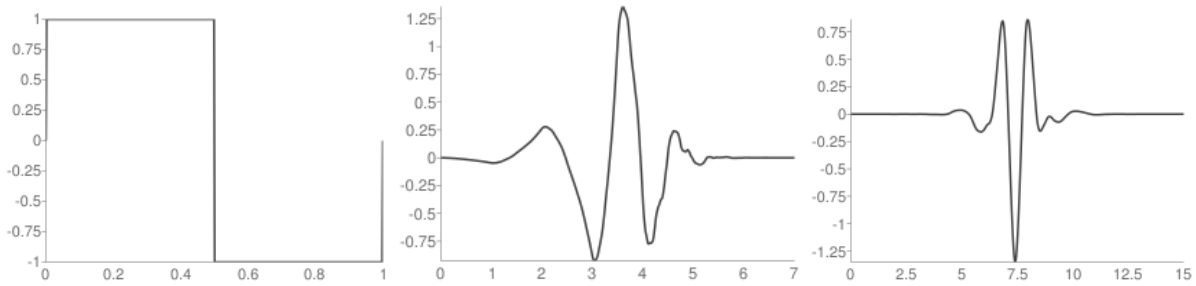

Figure 2.3: Wavelet Haar (haar), Wavelet Daubechies 4 (db4) and Wavelet Symlets 8 (sym8)

$$d + \lambda, \text{ for } d < \text{-} \lambda \qquad [34]$$

The primary principle behind wavelet denoising is to extract the ideal components of a signal from a noisy signal. This requires estimating the noise level.

In figure Figure 2.3, first one that shows the square shape is wavelet Haar, second figure shows the wavelet db4 and last one shows the daubechies least asymmetric wavelet known as symlets.

Now, Reconstruct the signal $\hat{x}_d(t)$ by taking inverse wavelet transform of the coefficient $W_{j,k}$ followed by: [32]

$$\hat{x}_d(t) = \mathrm{c}_\Psi \sum_{i=0}^{\infty} \sum_{k=-\infty}^{\infty} W_{j,k} \Psi_{j,k}(t)$$

Where, c_Ψ is the normalization constant followed by,

$$\mathrm{c}_\Psi = 1/(\int_{-\infty}^{\infty} (\frac{|\hat{\Psi}(W)|^2}{W}) dw) < \infty$$

Here, $\hat{\Psi}(W)$ is the Fourier transform of the wavelet function $\Psi(t)$.

To obtain clean signal , Integrate $\hat{x}_d(t)$ to yield the cleansed signal $\hat{x}(t)$ followed by:

$$\hat{x}(t) = \int \hat{x}_d(t) dt$$

There are several families of wavelets,e.g., haar, daubechies,biorthogonal, symlets, morlet, mexican Hat, etc. In this study, we have used haar,daubechies and symlets. Among of them, the use of Haar wavelet, Db4 wavelet and symlets8 is vast and these are shown in Figure 2.3.

The haar wavelet is an arrangement of rescaled "square-shaped" functions which together form a wavelet basis. The haar function (t) is a wavelet since it complies with all wavelet

requirements. Conceptually straightforward and memory-efficient due to its ability to be calculated locally without needing a temporary array, the haar wavelet transform has many benefits. It is also perfectly reversible, without the edge problems that face other wavelet transformations.

The mother wavelet function of the haar wavelet can be defined as:

$$\Psi(t) = 1 \text{ , if } 0 \leq \text{t} < 1/2$$

$$\text{-1 , if } \quad 1/2 \leq \text{t} < 1$$

$$0, \quad \text{otherwise} \qquad [35]$$

In comparison to the haar wavelet, the daubechies (db) wavelet is more complex. These wavelets are continuous, hence using them costs more in terms of computing than using the discrete haar wavelet. The db4 filter can be used to conduct the db wavelet transform. The signal can then be recreated using the wavelet coefficient and the inverse filter. The db4 wavelet transform is represented by the following filter equations.

1. $\text{a[n]} = \text{s[2n]} + \sqrt{3}S[2n+1]$

2. $\text{c[n]} = \text{s[2n]} + (\frac{\sqrt{3}}{4})a[n] \text{ - } (\frac{\sqrt{3}-2}{4})a[n-1]$

3. $\text{a[n]} = \text{a[n]} \text{ - } \text{c[n+1]}$

4. $\text{a[n]} = (\frac{\sqrt{3}-1}{\sqrt{2}})a[n]$

5. $\text{c[n]} = (\frac{\sqrt{3}+1}{\sqrt{2}})c[n] \qquad [35]$

For each wavelet transform iteration, these equations are applied sequentially. The signal array is stored in S, the low-pass coefficients are stored in a, and the high-pass coefficients are stored in c. The equations above can be reversed along with the actions they contain to produce the inverse db wavelet transform. As a result, the signal S can be denoised using the a and c coefficients.

Daubechies modified the db family by introducing the almost symmetrical wavelets known as symlets. Both wavelet families share comparable characteristics. This family has seven members (sym2 to sym8) and is also known as the daubechies least asymmetric wavelet.

Symlets have near-symmetric, orthogonal, and biorthogonal properties.

2.1.3 Empirical Mode Decomposition

EMD is a strategy for the investigation of non-stationary signals, which breaks down a signal into a whole of components. It breaks down any time series data into a limited set of zero that implies mono-components called intrinsic mode function (IMF). Using the Hilbert Transform, the characteristics of each component are analyzed. [8]

The time-frequency analysis can be carried out while staying in the time domain using empirical mode decomposition. EMD is a technique for decomposing a signal while remaining in the time domain, making it ideal for evaluating natural signals, which are frequently non-linear and non-stationary.

A multiscale signal, x (t), is adaptively decomposed by empirical mode decomposition (EMD) into a number L of what are known as intrinsic mode functions (IMFs),

$$h_i(t) \text{ , if } 1 \leq \text{i} < \text{L}$$

And

$$\text{x(t)} = \sum_{i=1}^{L} \text{h}_i(t) + \text{R(t)} \qquad [33]$$

When the remainder or residual, R(t), is a slowly varying function that doesn't have zero mean and has a small number of extrema.Due to the fact that all of the functions used to decompose signals are time-based and have the same duration as the original signal, varying frequencies in time can be preserved. While this type of data is almost undetectable in the Fourier domain or wavelet coefficients, it is obvious in an EMD analysis.

IMF is represented by two fundamental thoughts: [12]

- The number of zero-crossings and extrema either increases to or is only slightly different from one.
- The local extremes and minima that define the envelopes (waves) are zero.

The frequency content of the IMF drops as the level of the IMF rises. The curious truth about EMD is that it is highly adaptable and can extricate the non-stationary portion of the original function.

The first IMF contains almost nothing but noise with high frequency, and useful information about the signal components can be considered to be in rest of the IMFs,with the exception

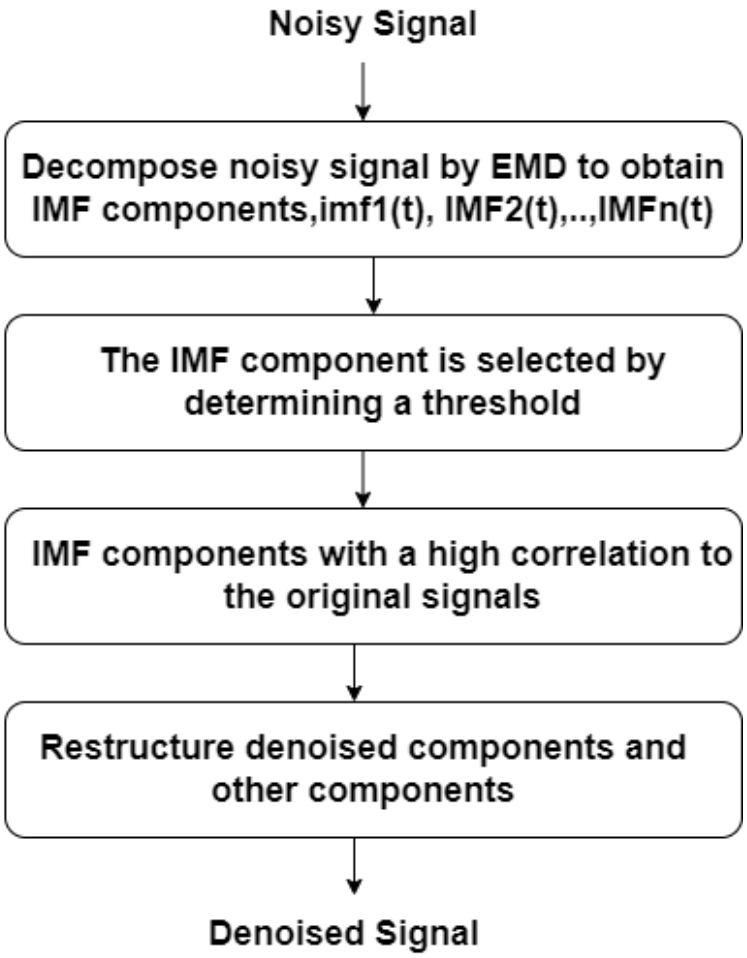

Figure 2.4: Block representation of Empirical Mode Decomposition (EMD) [40]

of the second IMF, which can be noisy. To reduce noise, it may be preferable to examine the total of the first two IMFs rather than the entire signal or only the first one. Along with the residue(R), the first two IMF components are calculated as signal,

$$x(n) = IMF_1(n) + IMF_2(n) + R(n).$$

It is possible to select the appropriate IMF or IMFs by examining the energy of this IMF in relation to the PPG signal since only in the noisy situation does the first IMF capture the noise.To find the appropriate IMF or IMFs adaptively, a threshold is determined from x(n). As a proportion of the maximum signal amplitude, this threshold or noise level (V_n) is computed as,

$$\mathrm{V}_n = \alpha(max(x(n))). \qquad Where, \alpha \text{ is a constant.}$$

The first IMF is the only factor taken into account to determine the connection with the signal until the first IMF falls below this threshold, at which point the signal has the proper amplitude. $IMF_1(n)$ samples n_L that lie between $-V_n$ to V_n are recognized as,

$$\mathrm{n}_L = \{t : t \epsilon n | IMF_1(t)| \leq \mathrm{V}_n\}$$

After using formula,

$$\mathrm{NLCR} = \frac{\sum_{n \epsilon n_L} IMF_1^2(n)}{\sum_{n \epsilon n_L} (X^2(n))}$$

the noise level crossing ratio (NLCR) is calculated. Finally, if this NLCR remains below or equal to a constant β the appropriate IMF is selected as sum of $IMF_1(n)$ and $IMF_2(n)$.If NLCR is greater than β then $IMF_1(n)$ is taken as the appropriate IMF. Here, β is a constant. Thus, the appropriate IMF component and the residue is the denoise signals.

2.2 Related Works

Mishra et al. [3] have work on different denoising techniques for PPG signals.This is a survey paper. The denoising technique of PPG signal is the agenda of segregation of corrupted or noisy signals from the original signal. PPG signals are usually affected by different artifacts. Power line interface, motion artifact (MA), Low amplitude PPG signal, premature ventricular contraction, and baseline wander (BW) are divergent types of noises that felonious the signal. To eliminate noise special filters have been used such as LMS filter, moving average filter, adaptive filters, Kalman filter, IMAR, Wavelets, median filter, notch filter, etc.This study presents an overview of numerous methods for PPG denoising based on different

forms of filtering, wavelet transform, empirical mode decomposition, independent component analysis, and cluster analysis.They have concluded that the AMARS-based filter and Motion Artifact removal of the artificial neural network-based technique performs well for minimizing baseline wander. They have given advice using the WPTICA-based approach to lessen powerline interference noise.

Reddy et al. [6] have used Fourier series exploration to diminish the effect of motion artifacts on pulse oximeter reading. When the patient is tied up with the oximeter, oxygen saturation (SpO2) is measured. Cycle-by-cycle Fourier series analysis has been used to extricat clean PPG from PPG signals corrupted by motion artifacts.The Fourier series is used on a cycle-by-cycle strategy to compensate for the quasiperiodic and non - stationarity nature of signals seen in a pulse oximeter. The experimental results demonstrate the usefulness of the cycle-by-cycle Fourier transformation and show that artifacts caused by a patient's movement are reduced by at least 35 dB. Using this transformation minimizes the error in SpO2 computation from 37% to 3% during periods of motion artifacts.

Alqaraawi et al. [8] proposed a probabilistic approach based on Bayesian learning. This technique is used to appraise HRV from PPG signals noted by wearable devices. The automatic multi-scale-based peak detection (AMPD) algorithm has been used to enhance the performance of peak detection in terms of sensitivity and positive predictive values.This algorithm focuses on to detect signal peaks by scrutinizing the local maxima scalogram (LMS) of periodic or quasi-periodic signals.Even when a signal contains white noise, the AMPD algorithm performs effectively. MATLAB simulation environment was used to handle and evaluate the captured PPG data.In terms of sensitivity and positive predictive values, they came to the conclusion that the probabilistic strategy based on Bayesian learning performed on the scale with the AMPD. In terms of ATR, it performs better than the AMPD.

Bashar et al. [15] has employed a machine learning approach using decision tree regression algorithm: Photoplethysmography (PPG) signal to measure heart rate. In this research paper, a multi-model machine learning approach (MMMLA) is petitioned to predict heart rate from wearable devices such as fingertip devices, and wrist-type devices. In this technique, K-means clustering has been used for splitting noisy and non-noisy data. After splitting, the separated data has been used to fit into the decision tree regression framework and measured the heart rate for test data. In this research, feature engineering has also been terminated. In feature engineering, a set of features have been chosen and investigated the behavior with different models.In order to estimate heart rate, they have calculated the root mean square (RMS) error and average absolute error. The researchers discovered that the absolute minimal inaccuracy is 1.18 beats per minute (BPM). The results of this work show that there is a good chance that the algorithm will be used to PPG-based HR monitoring.

To abolish motion artifacts from the PPG signal, a fast algorithm for heart rate estimation

based on a modified Spectral Subtraction Scheme Utilizing Composite Motion Artifacts Reference generation (SPECMAR)with two-channel PPG and three-axis accelerometer signals has been proposed by Islam et al. [16]. The motion artifact is seized by holding the minimum amplitude of each of the frequency bins of the three-channel accelerometer. Using this technique, an accurate heart rate is estimated so that significant noise reduction is achieved. SPECMAR method is having the potentiality to tracking the ground truth with high assessment accuracy. Therefore, it can be used in real-time applications which is unaccompanied by giving up estimation accuracy. Due to low reckoning complexity, the method is relatively faster than other methods. SPECMAR method is implemented in wearable devices because of the low estimation error, and smooth and fast heart rate tracing.

Ban et al. [17] proposed a movement noise cancellation algorithm for PPG signals using wide-band diversity and the wavelet transform. After measuring the PPG signals, the wavelet transform has been used to detect movement noise in the signals. PPG signals have been measured on many objects and different subjects.They came to the conclusion that this technique may minimize movement noise in PPG signals, which occurs in 30% of cases, to 5.18%. Although high-frequency noise can be filtered outThey have used the LAXTHA Inc. Ubpulse T1 at a sampling rate of 256 Hz to measure the PPG signal at various body parts, including the fingers and ears, in eight adults using a low pass filter movement noise cannot be canceled by a low pass filter because a nominal pulsatile has frequencies lower than 4 Hz.

Naraharisetti et al. [18] have compared various signal rectifying techniques used to reduce motion artifacts in this paper, including Adaptive Noise Cancellation (ANC), Wavelet Transform (WT), Independent Component Analysis (ICA), Singular Value Decomposition (SVD), and Cycle by Cycle Fourier series Analysis (FSA). .The PPG signal has been generated from MIT's MIMIC II waveform database (mimic2db), and the artifact PPG signal is from a44091c.They used MATLAB as the primary environment for developing these methods.They determined that SVD and FSA mechanisms lead to the greatest outcomes in terms of object segmentation after throwing the five policies into action.Both techniques have done a good job at heart rate estimation and artifact reduction.

Ismail et al. [19] have highly confidential motion artifacts in terms of signal-processing approaches and explored state-of-the-art techniques along with motion artifact removal and heart rate surveillance. Heart rate monitoring has been split into four categories signal decomposition-based trackers, signal subspace trackers, signal processing trackers, and machine learning trackers. This review report concludes that heart rate monitoring encompasses all of these interrelated domains. They have employed multi-resolution decomposition and adaptive filtering. For this review, they used the Respiration dataset, the Synthetic dataset, the IEEE SPC dataset, the Chon Lab dataset, the IEEE TBME Respiratory Rate Benchmark dataset, the BIDMC PPG dataset, and many others.

Li et al. [20] have used double median filters to offer a real-time denoising technique. Pulse oximeters and data acquisition operating systems were used to obtain the data. The high-frequency components of the signal through the first median filter were excluded using the boundary extension in order to prevent boundary distortion. The low-frequency components were approximated using the second median filter, and the estimated low-frequency components were then deducted from the signal. For the purpose of assessing the impacts of denoising, they have estimated the morphological distortions, frequency spectra, and signal-to-noise ratios (SNRs). They led to the conclusion that the SNR for noisy signals, wavelet-based techniques, and double median filters, respectively is 5.7739, 6.1874, and 11.3860.

Kasambe et al. [21] have suggested using a real-time VLSI Wavelet Transform denoising method to take the power line out of the PPG signal. For the purpose of evaluating the effectiveness of VLSI Wavelet-based PPG signal denoising, power line noise has been taken into account. Here, VLSI implementations have been used. The suggested wavelet-based denoising system is realized as a three-level decomposition-reconstruction tree. Additionally, mean absolute deviation and the standard deviation have been included as assessment criteria. Mean Absolute Deviation (MAD) and Standard Deviation have been computed (SD). They discovered that the MAD and SD for denoised signals in "Haar" were 1.976 and 2.457 and 0.478 and 0.392 for noisy signals, respectively.

Tabei et al. [22] have recommended the use of a probabilistic neural network idea using the specified extracted parameters. They have given consideration to MNAs that press their lenses, move their hands, and misplace their fingertip. Thirty volunteers have been instructed to move their hands in any direction, and five others to execute acts of fingertip misplacement MNAs in one set of measurements and lens-pressing MNAs in the other. This has been done in order to induce the hand movement MNA in a smartphone PPG recording.When selecting the performance indicators, they kept accuracy, sensitivity, and specificity in consideration. The results show that the customized MNA detection works better overall than the generalist technique. Accuracy, sensitivity, and specificity were attained at 89.92%, 84.21%, and 93.63% respectively.

Merry et al. [23] have discussed wavelet transformation. The main problem of Fourier transformation is, it retrieves only the global frequency content of the signal as a result information is lost. To overcome the problem they have used multi-resolution analysis of the local frequency content of a signal which is done by wavelet transformation. They have taken into account the change from the Fourier transform to the wavelet transform as indicated by the short-time Fourier transform (STFT).In this report, they have shown the different applications of wavelet transformation e.g. solving ordinary and partial differential equations, Real-time feature detection, Motion detection and tracking, signal denoising, nonlinear adaptive wavelet control,Audio structure decomposition, determining both linear

and nonlinear control objectives, etc.

Lei et al. [24] have proposed a system combining the unconventional component analysis and the non-negative matrix factorization with complementary ensemble empirical mode decomposition to separate the PPG signal into two sets of signals as well as the principal component analysis to generate two surrogate signals. They have estimated both the heart rate and the respiratory rate from the PPG signal. The advantage of this strategy is to diminish the reconstruction error. They have used the Medical Information Mart for rigorous Care database as the dataset. They have achieved 99.96%, and 98.79% accuracy for heart rate and respiratory rate respectively.

Karim et al. [25] have used Empirical Mode Decomposition to remove the motion artifact and reconstruct a clean PPG signal. They have completed two stages of work. The first is the monitoring of the PPG signal, and the second is the identification of the ECG signal peak.They have utilized a heartbeat oximeter to collect PPG signals from various human body areas and collected data from twelve males with extended ages from 18-35 during the physical exercises.The spectral subtraction technique has been used to remove noise from the signal. This method evaluates and subtracts from the average signal spectrum and average noise spectrum. Signal-to-noise ratio (SNR) can be increased in this way.Because machine learning is used for prediction, it is an effective strategy to eliminate Motion artifacts.They have concluded that using Linear Regression Classifier (LRC) the model has anticipated 93% of information accurately.

Tang et al. [26] have recommended the use of the Empirical Mode Decomposition (EMD) taken after by Discrete Wavelet Transform (DWT) to reduce noise from the PPG signal. They have collected information from the IEEE Signal Processing Cup competition dataset. Raw PPG signals have been collected from the wrist device using two pulse oximeters with green LEDs. They have achieved 15.14 BPM Mean Sum Error (MSE) using only DWT whereas 10.43 bpm MSE and 12 bpm Absolute Maximum Error (AME) have achieved using both EMD and DWT.They have demonstrated that the heartbeat rate detection is improved for 67% of the datasets when using a combination of EMD and DWT filters to rebuild the PPG signals.

Sun et al. [[27] have tried to suggest a processing protocol based on Hilbert transform and empirical mode decomposition (EMD) to alleviate the contamination of motion artifacts and increase the accuracy of heartbeat identification in PPG. For the desired outcome of accurate and consistent heart rate extraction, a signal processing technique based on multi-scale data analysis and employing empirical mode decomposition (EMD) has been outlined in this study. With a final recovery rate of 84.68%, tests using signals from the Physionet database and the signals demonstrate how their technology might boost the accuracy of heartbeat detection.

Motin et al. [28] have thoroughly investigated how each EMD redistributive the removal of BR from PPG. In order to extract BR from PPG, they employed an EMD family PCA-based hybrid model, which is a logical progression from the ensemble EMD (EEMD) PCA hybrid model that was previously manufactured. Using the MIMIC and Capnobase datasets, two distinct models' performance has been evaluated. For the MIMIC and Capnobase datasets, the median absolute error ranged from 0 to 5.03 and 2.47 to 10.55 breaths/min, respectively. The suggested method comprises three phases: (1) Data Pre-Processing and Decomposition, (2) Determination of IMFS and Dismissals of Artifacts, and (3) Extraction of Breathing Rate.

Chapter 3

Methodology

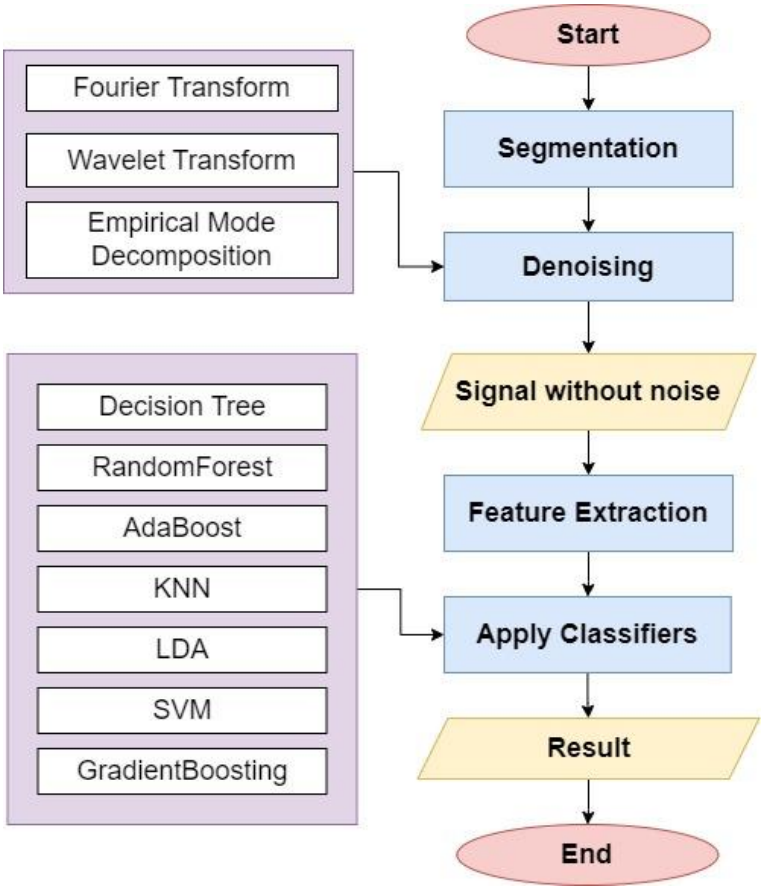

Figure 3.1: Entire process of the work

We first segment the signal for each of the three methods.The segmented signals are then subjected to the denoising procedures. The next step was to extract features from this processed signal.We then use 7 lightweight classifiers which are available on low-power wearable devices to measure performance on stress detection.Figure 3.1 shows our entire working procedure.

3.1 Dataset and Attributes

Long-term stress is recognized to have negative effects on wellbeing, necessitating the use of automated systems for monitoring stress on a constant basis. There aren't any widely used standard datasets for detecting an individual's affective state based on observables in the affective computing community. Therefore, we have used WESAD, a publicly available dataset for wearable stress and affect detection. This multimodal dataset contains physiological and mobility data from 15 people that were collected during a lab experiment using both a wrist and a chest-worn device. Blood volume pulse (BVP), electrocardiogram (ECG), electrodermal activity (EDA), electromyogram (EMG), respiration (RESP), body temperature (TEMP), and three-axis acceleration(ACC) are among the sensor modalities that are included in this dataset. Hence attributes of this dataset are BVP, ECG, EDA, EMG, RESP, TEMP, and ACC. Additionally, the dataset includes subject self-reports that were gathered via a number of standard questionnaires. They were able to achieve classification accuracy of up to 80% using this dataset and the three-class classification problem (baseline, stress, and amusement). Accuracy levels of up to 93% were achieved in the binary scenario (stress vs. non-stress).

3.2 Fourier Transform

In the Fourier transform, we have used a statistical method to remove noisy segments of signals in terms of time. At first, we apply a fast Fourier transform on PPG signals. The next step was to identify frequency components corresponding to the noisy signal. To do so, we extracted the valley from noisy signals and per cycle divided it into segments. The basic moving-window method has a problem with inaccurate valley recognition because noise causes all signals to continuously identify false valleys.To resolve this issue, the mean of the total signal's amplitude has been determined, along with set segments from the previous to the current points. Each segment contains mean values of the amplitude of the entire signal. We have calculated the standard deviation, kurtosis, and skewness of all segmented data using the following expressions:

$$\text{Standard deviation, } \sigma = \sqrt{\frac{1}{n}\sum_{i=0}^{n}(x_i - \bar{x})^2}$$

$$\text{Kurtosis} = \frac{\frac{1}{n}\sum_{i=1}^{n}(x_i - \bar{x})^4}{std^4}$$

$$\text{Skewness} = \frac{\frac{1}{n}\sum_{i=1}^{n}(x_i - \bar{x})^3}{std^3}$$

Here, σ stands for standard deviation and $\bar{x}$ is for mean value.

We have calculated the threshold $T_\sigma, T_k, and T_{s1}$ using the following expression:

$$\mathrm{T}_\sigma = \bar{\sigma} + \alpha \qquad , T_k = \bar{k} + \beta \qquad and$$

$$\mathrm{T}_{s1} = \bar{s} - \gamma \qquad , T_{s2} = \bar{s} + \delta$$

Here, $\bar{\sigma}$, $\bar{k}$, and $\bar{s}$ represents standard deviation, kurtosis, and skewness, respectively. The values of optimal parameters are:

$\alpha = 1.0, \beta = 2.0, \gamma = 1.8, and \delta = 1.5$

Removing all the segments beyond the threshold, we have reconstructed the signal. Finally, for smoothing the final signal we have used a moving average filter.

In order to find the ultimate peak point, we subjected the ensemble to five peak-detecting techniques, including LMM, BGM, FDA, SFA, and MAD.

Local maxima method (LMM): This technique takes the signal's local points and extracts them all, discarding any points with values below the average of the signal's amplitude.

Block generation with the mean of the signal threshold method (BGM): Blocks containing the mean values of the signal's amplitude are generated using this procedure. Each block's biggest values are contained in the peak point.

First derivative with an adaptive threshold method (FDA): Using this method, the signals are differentiated and the points with differential values of zero are considered peak candidates. Here, we have considered the peak point which peaks candidates with a larger amplitude than the threshold. We have set the threshold by applying a selective window.

Slope sum function with an adaptive threshold method (SFA): With this technique, the changed signal is processed to extract all local points. In order to achieve this, we have only kept ascending points throughout the differential process, setting the remaining points to zero. Only those points whose amplitudes exceeded the threshold were retrieved. The adjusted signal's ultimate peak point may be seen in the retrieved peak points. Enhancing the PPG pulse's upward slope and covering the rest of the pressure waveform are the slope sum function's main goals.

Moving averages with the dynamic threshold method (MAD): We have taken the square of all signals and placed signals below zero. As a result, two moving averages produce the block. The biggest amplitude point has evolved as the peak point in each exerted block.

PPG sensors are widely used to measure heart activities. HRV which has become the indicator of disease conditions, requires an accurate estimation of the time interval between successive peaks in the PPG signal. To calculate HRV, the signal must be split up into accurate window sizes. At least two minute window length is required to extract all the features accurately. To extract HRV features we have used 2 minute of window length and 0.25sec

Table 3.1: List of extracted features

Domain	Parameter	Description	Unit
Time	Mean HR	Mean HR	$\frac{1}{min}$
	Std HR	Standard deviation of the HRs	$\frac{1}{min}$
	MeanNN	Mean of N-N intervals	ms
	SDNN	Standard deviation of N-N intervals	ms
	MedNN	Median of N-N intervals	ms
	MeanSD	Mean of successive N-N interval differences	ms
	SDSD	Standard deviation of successive N-N interval differences	ms
	RMSSD	Root mean square of successive N-N interval differences	ms
	pNN20	Percentage of successive N-N intervals that differ by more than 20ms	%
	pNN50	Percentage of successive N-N intervals that differ by more than 50ms	%
	TINN	Baseline width of the R-R interval histogram	M s
Frequency	LF	Power in the low-frequency band(0.04 - 0.15Hz)	ms^2
	HF	Power in the high-frequency band(0.15 - 0.4Hz)	ms^2
	LF/HF	Ratio of LF to HF	
	ULF	Power in the ultra-low-frequency band(0.003Hz)	ms^2
	VLF	Power in the very-low-frequency band(0.003 - 0.04Hz)	ms^2
	P(TotPow)	Total power 0.003-0.4Hz	ms^2
	LF/P	Ratio of low-frequency to total power	-
	HF/P	Ratio of high frequency to total power	-
Non-Linear	SD1	Poincare plot standard deviation perpendicular to the line of identity	M s
	SD2	Poincaré plot standard deviation along the line of identity	M s
	pQ	pQ = SD1 / SD2	-
	pA	pA = SD1 * SD2	ms^2
	ApEn	Approximate entropy	-
	ShanEn	Shannon entropy	-
	D2	Correlation dimension, which estimates the minimum number of variables	-

of the sliding window. All the peak points are not perfectly extracted so there exists an inaccurate interval between successive peaks. To solve this problem, we have eliminated approximately 300 ms greater or lesser than the mean of entire intervals, the rest used for HRV feature extraction. To extract the HRV feature, we have used the HRV time domain, frequency domain, and non-linear domain. The features we have used are listed in Table 3.1.To measure the performance of stress detection, we used seven popular learning-based classifiers.The effectiveness of each denoising approach was evaluated using the area under the receiver operating characteristic curve(AUC) and F1 score. The performance of the present approach and the denoising methods were compared using accuracy.In this study, the data set is separated into two parts: training and testing data with a split ratio of 80:20.

3.3 Wavelet Transform

For wavelet transform, a 2-minute sliding window with a 0.25s sliding step was applied to segment the signal data following the recommendation by Kreibig et al. [34]. Furthermore, for each sensor's data, we created six different signals: the original signal, its first and second derivatives, and the transformed signal data using a Discrete Wavelet Transform (DWT) at three different frequencies (1 Hz, 2 Hz, and 4 Hz). We have used three different wavelets from 3 different families here. They are- haar,db4, and sym8.Frequency and time information can be collected by wavelet transformations, and the mother wavelet can capture abrupt changes in signals [35]. Besides the 3-dimensional signal data (x, y, and z-axis that is represented by ACC_x,ACC_y, and ACC_z, respectively), we also computed their magnitude (ACC_{norm})using Equation (1) for the ACC data. As shown in Table 3.2, we have employed signals including six TEMP signals, twenty-four ACC signals, six EDA signals, and six BVP signals.

$$\text{ACC}_{norm} = ACC_x^2 + ACC_y^2 + ACC_z^2$$

Next, we denoise these signals by soft thresholding with a BayesShrink approach. Both positive and negative coefficients are being shrunk toward zero for soft thresholding. A distinct threshold is estimated for each wavelet subband in the adaptive wavelet soft thresholding method known as BayesShrink. This typically yields better results than those that can be obtained using a single threshold.

After that, we extracted 10 statistical features from the denoised signals using BioSPPy and Numpy libraries [37] in Python as displayed in Table 3.3. In total, 420 features were analyzed for this study. To measure the performance of stress detection, we used seven popular learning-based classifiers. In this study, the data set was divided into two parts: training and testing data with a split ratio of 80:20. All the strategies use the training data

Table 3.2: Signal data used in wavelet transform and EMD

Sensor	**Signal**
Skin Temperature(ST)	ST original signal ST first derivative signal ST second derivative signal ST signal with DWT at 4 Hz,2Hz,1Hz
Accelerometers(ACC)	ACC_x original signal ACC_x first derivative signal ACC_x second derivative signal ACC_x signal with DWT at 4 Hz,2Hz,1Hz ACC_y original signal ACC_y first derivative signal ACC_y second derivative signal ACC_y signal with DWT at 4 Hz,2Hz,1Hz ACC_z original signal ACC_z first derivative signal ACC_z second derivative signal ACC_z signal with DWT at 4 Hz,2Hz,1Hz ACC_{norm} original signal ACC_{norm} first derivative signal ACC_{norm} second derivative signal ACC_{norm} signal with DWT at 4 Hz,2Hz,1Hz
Electrodermal Activity(EDA)	EDA original signal EDA first derivative signal EDA second derivative signal EDA signal with DWT at 4 Hz,2Hz,1Hz
Blood volume pulse sensor(BVP)	BVP original signal BVP first derivative signal BVP second derivative signal BVP signal with DWT at 4 Hz,2Hz,1Hz

Table 3.3: Statistical features for wavelet transform and EMD

1	Mean of the Signal
2	Minimum value of the signal
3	Maximum value of the signal
4	Median of the signal
5	Maximum signal amplitude
6	Signal variance
7	Standard signal deviation
8	Absolute signal deviation
9	Signal kurtosis
10	Signal skewness

for training and testing data to evaluate the performance. Several measurements including Accuracy (Acc), F1-score (F1), and AUC were deployed for classifier performance.

3.4 Empirical Mode Decomposition

For empirical mode decomposition, the signal data were also segmented by using a 2-minute sliding window with a sliding step of 0.25 s. Then we preprocessed segmented data in 2 steps- we handle drift suppression using a high pass filter and high-frequency suppression using a low pass filter. There may still be some high-frequency noise in the signal even after preprocessing and filtering. These noises would be represented by the first IMF component in such circumstances. We have applied the method outlined in [38] to determine whether the first IMF component includes useful information or is just noise.

In order to denoise, we perform the following steps:

1. Empirical Mode Decomposition is performed on the filtered signal and the first two IMF components along with the residue are computed as follows:

$$\mathrm{x(n)} = \mathrm{IMF}_1(n) + IMF_2(n) + R(n)$$

Where,

x(n) = Filtered Signal
$\mathrm{IMF}_1(n) = 1st\ \ IMF\ \ component$
$IMF_2(n) = 2nd\ \ IMF\ \ component$
$R(n) = Residue$

2. The noise level (V_n) is calculated as a percentage of the maximum signal amplitude as follows:

$$\mathrm{V}_n = \alpha(max(x(n)))$$

Where, α is a constant that should be chosen wisely. We took $\alpha = 0.05$.

3. The samples $n_L$of IMF1(n) that falls within $-V_n$ to V_n are identified, i.e.,

$$\mathrm{n}_L = \{t : t \epsilon n | IMF_1(t)| \leq \mathrm{V}_n\}$$

4. The noise level crossing ratio (NLCR) is calculated using the following formula,

$$\mathrm{NLCR} = \frac{\sum_{n \epsilon n_L} IMF_1^2(n)}{\sum_{n \epsilon n_L} (X^2(n))}$$

5. Finally, the appropriate IMF is selected as follows :

$$\mathrm{IMF} = \mathrm{IMF1(n)} + \mathrm{IMF2(n)}, \text{ if NLCR} \leq \beta.$$

$$\mathrm{IMF1(n)} \text{ , otherwise.}$$

Here, β is a properly chosen constant. The β value we used was 0.02. Thereby, for feature extraction, the appropriate IMF component and residue are used. We extracted 10 statistical features from the IMF component and the residue using BioSPPy and Numpy libraries [37] in Python as displayed in Table 3.3. In total, 420 features were analyzed for this study. Lastly, we used seven popular learning-based classifiers.The data set used in this study was divided into two groups training data and testing data, with a split ratio of 80:20. For training the classifiers, each strategy has used training data and testing data for assessing the performance. For classifier performance, a number of metrics, including Accuracy (Acc), F1-score (F1), and AUC, were used.

Chapter 4

Experimental Result

4.1 Experimental Setup

WESAD provides various biological signals and three emotional states: baseline, stress, and amusement, are listed [5]. The baseline condition represents a neutral affective state. We have used only a single PPG signal with a 64 Hz sampling rate. To determine the cut-off and threshold for the noise-elimination procedure, a reference signal that was derived from a 0.1% high-quality signal with high peak detection performance was used.The feature extraction process produced 952 windows. To see the stress detection performance seven typical learning-based classifiers were used [5], [14]. They are: Decision tree, Random forest, AdaBoost, k nearest neighbor(KNN), Linear discriminant, Support Vector Machine(SVM), and gradient boosting. To compare performance between the existing method and the proposed method we used accuracy. And to measure the proposed method's performance the area under the receiver operating characteristic curve (AUC) [6] and F1 scores were used.

4.2 Performance of Fourier Transform

Table 4.1 presents the results of each classifier for fourier transform. The AUC and F1 scores of each of the seven classifiers are listed in this table. The best outcome was obtained by the Linear Discriminant Analysis (LDA) classifier, which had an AUC of 93.11 and an F1 score of 90.59.Decision tree classifier has relatively poor performance for Fourier transform.It had an AUC of 90.32 and an F1 score of 86.54.Among the seven classifiers, these are the lowest values.

Table 4.1: Summary of the performance of Fourier transform with seven classifiers

	Decision tree	**Random forest**	**AdaBoost**	**KNN (K=9)**	**LDA**	**SVM**	**Gradient boosting**	**Average**
AUC	90.32	90.74	90.99	92.20	93.11	92.28	91.59	91.70
F1	86.54	87.47	87.91	88.10	90.59	88.99	88.99	88.37

Table 4.2: Summary of the performance of peak detecting methods with seven classifiers regarding Fourier transform

Peak detecting methods	**Decision tree**	**Random forest**	**AdaBoost**	**KNN (K=9)**	**LDA**	**SVM**	**Gradient boosting**	**Average**
	AUC(F1 score)							
LMM	78.68 (67.15)	82.83 (74.38)	81.86 (72.27)	81.39 (70.50)	81.55 (70.60)	84.60 (76.48)	83.94 (76.01)	82.12 (72.48)
BGM	86.42 (81.43)	88.50 (83.44)	91.28 (87.72)	89.73 (84.11)	92.08 (89.13)	91.30 (87.30)	90.32 (86.94)	89.94 (85.72)
FDA	87.47 (81.04)	89.14 (84.47)	88.93 (83.71)	90.34 (85.37)	92.07 (88.03)	91.18 (86.99)	90.99 (86.71)	90.06 (85.19)
SFA	82.48 (74.44)	87.47 (81.77)	88.69 (83.07)	87.36 (81.19)	91.65 (87.81)	91.49 (87.39)	89.34 (83.97)	88.35 (82.80)
MAD	85.35 (78.34)	89.02 (84.62)	88.37 (84.06)	90.79 86.99)	93.81 (91.18)	92.69 (89.36)	91.58 (87.66)	90.23 (86.03)
ENS	90.32 (86.54)	90.74 (87.47)	90.99 (87.91)	92.21 (88.10)	93.22 (90.59)	92.83 (88.99)	91.59 (88.99)	91.70 (88.37)

4.3 Performance of Peak Detection Methods

To compare the peak detection methods' performance we use 5 different peak detection methods and then ensemble them. These 5 methods are - Local maxima method (LMM), Block generation with the mean of the signal threshold method (BGM), First derivative with an adaptive threshold method (FDA), Slope sum function with an adaptive threshold method (SFA), Moving averages with the dynamic threshold method (MAD). We have applied these methods after noise filtering and elimination of the signal. In Table 4.2, we can see the peak detection methods performance result by averaging all the results of the seven classifiers of AUC and F1 scores. Ensemble-based peak detection method has the best result with 91.70% for AUC and 88.37% for the F1 score.

Table 4.3: Summary of the performance of three mother wavelets with seven classifiers regarding wavelet transform

		Decision tree	**Random forest**	**AdaBoost**	**KNN (K=9)**	**LDA**	**SVM**	**Gradient boosting**	**Average**
Haar	AUC	99.95	95.12	99.77	99.99	96.78	94.76	99.91	98.04
	F1	99.95	93.86	99.74	99.98	96.29	93.38	99.90	97.58
DB4	AUC	99.92	93.12	99.64	99.95	96.11	94.12	99.92	97.54
	F1	99.88	91.40	99.44	99.94	95.41	92.59	99.99	99.95
Sym8	AUC	99.92	93.38	99.72	99.95	96.71	95.18	99.93	97.83
	F1	99.91	92.45	99.64	99.93	96.06	94.05	99.90	97.42

4.4 Performance of Wavelet Transform

The results of each classifier for wavelet transform with three different mother wavelet is presented in Table 4.3. This table lists the AUC and F1 scores of each of the seven classifiers.Haar has the best performance with an average 98.04 for AUC and 97.58 for F1 score. The decision tree classifier has more than 99% AUC and F1 score for all the three mother wavelets.

Table 4.4: Summary of the performance of EMD with seven classifiers

	Decision tree	**Random forest**	**AdaBoost**	**KNN (K=9)**	**LDA**	**SVM**	**Gradient boosting**	**Average**
AUC	99.75	90.36	91.78	85.02	83.98	60.35	96.36	86.79
F1	99.60	85.22	87.91	79.96	76.90	33.09	95.25	79.70

4.5 Performance of EMD

Table 4.4 presents the results of each classifier for empirical mode decomposition. Each of the seven classifiers' AUC and F1 scores is listed in this table. The best outcome was obtained by the decision tree classifier, which had an AUC score of 99.70 and an F1 score of 99.60.SVM's performance for EMD is the worst. It has an AUC score of 60.35 and an F1 score of 33.09.

4.6 Comparison of the Performance of the Three Denoising Methods with the Current Method

In this Figure 4.1, we have shown the barchart of F1-score comparison of the performance of the three denoising methods with the current method and Table 4.5 presents the overall performance with the value of Accuracy and F1-score of the three denoising methods with the current method proposed by Schmidt, Philip, et al under the same conditions [9] .We used the same methodology as the prior way to measure the accuracy and F1 score [9]. The five classifiers achieved a performance improvement at an average accuracy of 7.86% and F1 score of 7.80%, demonstrating that our three techniques outperform the prior method. Among the three of our methods, wavelet transform has the best performance. It has the maximum accuracy and f1 score for all of the seven classifiers.

Table 4.5: Comparison of the Performance of the three denoising methods with the current method

	Decision tree	**Random forest**	**AdaBoost**	**KNN (K=9)**	**LDA**
	Accuracy(F1 score)				
Philip et al [9],	81.39 (78.27)	84.18 (81.35)	84.10 (81.23)	82.06 (78.94)	85.83 (83.08)
Fourier Transform	90.75 (86.54)	91.57 (87.47)	91.62 (87.91)	88.11 (88.10)	94.79 (90.59)
Wavelet Transform	99.97 (99.95)	96.82 (93.86)	99.84 (99.74)	99.97 (99.98)	98.00 (96.29)
Empirical Mode decomposition	99.76 (99.60)	92.96 (85.22)	93.52 (87.91)	88.26 (79.96)	89.45 (76.90)

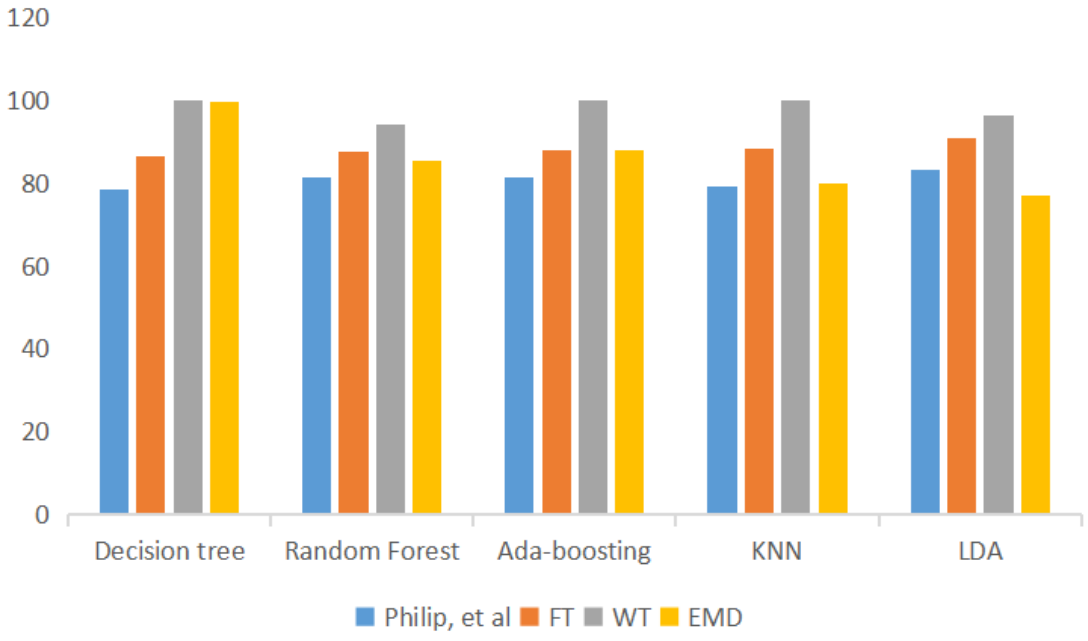

Figure 4.1: F1-Score comparison of the three denoising methods with the current method

Chapter 5

Conclusion And Future Work

5.1 Conclusion

As denoising approaches for stress detection in our study, we have used the Fourier transform, Wavelet transform, and empirical mode decomposition. To enhance the efficacy of stress identification in Fourier, we have employed an ensemble-based peak-detection technique. This integrated approach outperformed the previous strategy with numerous classifiers in terms of stress detection. For each sensor's data in wavelet, the signal data were split by a sliding window of 0.25s and six distinct signals were created. These signals were denoised using soft thresholding and a BayesShrink method, and 10 statistical features were then retrieved using BioSPPy from the denoised signals. The data-adaptive method empirical mode decomposition(EMD) breaks down a signal into constituents known as intrinsic mode functions (IMFs). After denoising, the relevant IMF component and the residue are selected for feature extraction, and 10 statistical features were extracted using BioSPPy from the IMF component and the residue. We also looked at the PPG signal's results both before and after applying the denoising techniques. In comparison to the Fourier transform and empirical mode decomposition, the wavelet transform offers better performance and is more effective in handling time-frequency analysis.

5.2 Future Work

We have used Fourier transform, wavelet transform and EMD to denoise the PPG signal and got experimental results as regards. EEG(popularly known as brain waves), and ECG are some other biosignal which are frequently used as biomedical indicators. Diagnosis of various illnesses is done by analyzing these biomedical signals. In the future we will try to denoise EEG and ECG signals using Fourier transform, wavelet transform and EMD to see which one gives the best result.

References

[1] T. Fawcett,"An introduction to ROC analysis," Pattern Recognit. Lett., vol. 27, no. 8,pp. 861874, Jun. 2006, doi: https://doi.org/10.1016/j.patrec.2005.10.010

[2] P. V. Kasambe, and S. S. Rathod,"VLSI wavelet based denoising of PPG signal." Procedia Computer Science,vol.49, pp.282-288,2015. doi: https://doi.org/10.1016/j.procs.2015.04.254

[3] B. Mishra and N. S. Nirala, "A Survey on Denoising Techniques of PPG Signal," 2020 IEEE International Conference for Innovation in Technology (INOCON),pp. 1-8, 2020, doi: https://doi.org/10.1109/INOCON50539.2020.9298358.

[4] K.Kabitha, S.Vasuki, and B.Karthikeyan,"PPG Signal Denoising using a New Method for the Selection of Optimal Wavelet Transform Parameters," Journal of University of Shanghai for Science and Technology,vol.23,Oct 21.

[5] J. Zhai and A. Barreto, "Stress detection in computer users through noninvasive monitoring of physiological signals," Biomed Sci Instrum,vol.42, pp.495-500,2006,PMID:16817657.

[6] K. A. Reddy, B. George and V. J. Kumar," Use of Fourier Series Analysis for Motion Artifact Reduction and Data Compression of Photoplethysmographic Signals," in IEEE Transactions on Instrumentation and Measurement, vol. 58, no. 5, pp. 1706-1711, May 2009, doi: https://doi.org/10.1109/TIM.2008.2009136.

[7] M. Elgendi, I. Norton, M. Brearley, D. Abbott, D. Schuurmans, "Systolic peak detection in acceleration photoplethysmograms measured from emergency responders in tropical conditions," PLoS One,vol. 8,Oct 22 2013, doi: https://doi.org/10.1371/journal.pone.0076585 PMID:24167546;PMCID: PMC3805543.

[8] A. Alqaraawi, A. Alwosheel, and A. Alasaad ,"Heart rate variability estimation in photoplethysmography signals using Bayesian learning approach," Healthcare technology letters, vol.3(2), pp.136–142,Jun 2016, doi: https://doi.org/10.1049/htl.2016.0006

[9] P. Schmidt, A. Reiss, R. Duerichen, C. Marberger, and K. Van Laerhoven, "Introducing WESAD, a multimodal dataset for wearable stress and affect detection," in Proc. 20th ACM Int. Conf. Multimodal Interact.,pp. 400408, Oct. 2018, doi: https://doi.org/10.1145/3242969.3242985

[10] S. Heo, I. Kim, S. Kwon, H. Lee, and J. Lee, "PPG signal preprocessing and comparison study with learning-based model for stress detection," J. Korean Inst. Commun. Sci.,pp. 595596, Aug. 2020

[11] S. Heo, S. Kwon and J. Lee, "Stress Detection With Single PPG Sensor by Orchestrating Multiple Denoising and Peak-Detecting Methods," in IEEE Access, vol. 9, pp. 47777-47785, 2021, doi: https://doi.org/10.1109/ACCESS.2021.3060441.

[12] E. Harikrishna, and K. A. Reddy, "Use of Transforms in Biomedical Signal Processing and Analysis", in Real Perspective of Fourier Transforms and Current Developments in Superconductivity. London, United Kingdom: IntechOpen, May, 2021. doi: https://doi.org/10.5772/intechopen.98239

[13] Yi-Hsiang Yang and Kea-Tiong Tang, "A pulse oximetry system with motion artifact reduction based on Fourier analysis," 2014 IEEE International Symposium on Bioelectronics and Bioinformatics (IEEE ISBB 2014), 2014, pp. 1-4, doi: https://doi.org/10.1109/ISBB.2014.6820902.

[14] A. Esmaili, M. Kachuee and M. Shabany, "Nonlinear Cuffless Blood Pressure Estimation of Healthy Subjects Using Pulse Transit Time and Arrival Time," in IEEE Transactions on Instrumentation and Measurement, vol. 66, no. 12, pp. 3299-3308, Dec. 2017, doi: https://doi.org/10.1109/TIM.2017.2745081.

[15] S. S. Bashar, M. S. Miah, A. H. M. Z. Karim and M. A. Al Mahmud, "Extraction of Heart Rate from PPG Signal: A Machine Learning Approach using Decision Tree Regression Algorithm," 2019 4th International Conference on Electrical Information and Communication Technology (EICT), 2019, pp. 1-6, doi: https://doi.org/10.1109/EICT48899.2019.9068845

[16] M.T. Islam, S.T. , Ahmed, C. Shahnaz, et al. "SPECMAR: fast heart rate estimation from PPG signal using a modified spectral subtraction scheme with composite motion artifacts reference generation," Med Biol Eng Comput 57, pp. 689–702 ,2019. doi: https://doi.org/10.1007/s11517-018-1909-x

[17] D. Ban and S. Kwon, "Movement noise cancellation in PPG signals," 2016 IEEE International Conference on Consumer Electronics (ICCE), 2016, pp. 47-48, doi: https://doi.org/10.1109/ICCE.2016.7430517.

[18] K. V. P. Naraharisetti and M. Bawa, "Comparison of different signal processing methods for reducing artifacts from photoplethysmograph signal," 2011 IEEE INTERNATIONAL CONFERENCE ON ELECTRO/INFORMATION TECHNOLOGY, 2011, pp. 1-8, doi: https://doi.org/10.1109/EIT.2011.5978571.

[19] S. Ismail, U. Akram and I. Siddiqi, "Heart rate tracking in photoplethysmography signals affected by motion artifacts: a review". EURASIP Journal on Advances in Signal Processing, 2021(1),pp.1-27, doi: https://doi.org/10.1186/s13634-020-00714-2

[20] S. Li, L. Liu, J. Wu, B. Tang, D. Li, "Comparison and Noise Suppression of the Transmitted and Reflected Photoplethysmography Signals". Biomed research international, 2018, doi: https://doi.org/10.1155/2018/4523593.

[21] P.V. Kasambe, and S.S. Rathod, 2015. "VLSI wavelet-based denoising of PPG signal." Procedia Computer Science, 49, pp.282-288, doi: https://doi.org/10.1016/j.procs.2015.04.254.

[22] F. Tabei, R. Kumar, T.N. Phan, D.D. McManus, and J.W. Chong, "A Novel personalized motion and noise artifact (MNA) detection method for smartphone photoplethysmograph (PPG) signals." IEEE Access, 6,pp.60498-60512, 2018, doi: https://doi.org/10.1109/ACCESS.2018.2875873.

[23] R.J.E. Merry, and M. Steinbuch, "Wavelet theory and applications." literature study, Eindhoven university of technology, Department of mechanical engineering, Control systems technology group, 2005, doi: https://doi.org/10.1007/978-1-4419-1545-0.

[24] R. Lei, B.W.K. Ling, P. Feng, and J. Chen, "Estimation of heart rate and respiratory rate from ppg signal using complementary ensemble empirical mode decomposition with both independent component analysis and non-negative matrix factorization." Sensors, 20(11),p.3238, 2020, doi: https://doi.org/10.3390/s20113238.

[25] A.Z. Karim, M.A. Al Mahmud, M.S. Miah, S.S. Bashar, S. Oh, J. Kim, and M. Marium, "Peak Detection and Tracking of PPG Signal: A Multi-model approach using Empirical Mode Decomposition Machine Learning." The Journal of Contents Computing, 2(2),pp.153-163, 2020. doi: https://doi.org/10.9728/JCC.2020.12.2.2.153

[26] S.D. Tang, Y.S. Goh, M.D. Wong, and Y.E. Lew, "PPG signal reconstruction using a combination of discrete wavelet transform and empirical mode decomposition." In 2016

6th International Conference on Intelligent and Advanced Systems (ICIAS) (pp.1-4).IEEE, 2016 August, doi: https://doi.org/10.1109/ICIAS.2016.7824118

[27] X. Sun, P. Yang, Y. Li, Z. Gao and Y.T. Zhang, "Robust heartbeat detection from photoplethysmography interlaced with motion artifacts based on empirical mode decomposition." In Proceedings of 2012 IEEE-EMBS International Conference on Biomedical and Health Informatics (pp. 775-778). IEEE, 2012, January. doi: https://doi.org/10.1109/BHI.2012.6211698

[28] Motin, M.A., Karmakar, C.K. and Palaniswami, M., "Selection of empirical mode decomposition techniques for extracting breathing rate from PPG." IEEE Signal Processing Letters, 26(4),pp.592-596, 2019. doi: https://doi.org/10.1109/LSP.2019.2900923

[29] Raghuram, M., Madhav, K.V., Krishna, E.H. and Reddy, K.A., "Evaluation of wavelets for reduction of motion artifacts in photoplethysmographic signals. In 10th International Conference on Information Science, Signal Processing and their Applications (ISSPA 2010) (pp. 460-463). IEEE., 2010, May. doi: https://doi.org/10.1109/ISSPA.2010.5605443

[30] L.M.B. Alonzo, and H.S. Co, "Ensemble Empirical Mode Decomposition of Photoplethysmogram Signals in Biometric Recognition." In 2019 4th Asia-Pacific Conference on Intelligent Robot Systems (ACIRS) (pp. 255-259). IEEE, 2019, July., doi: https://doi.org/10.1109/ACIRS.2019.8935943

[31] W. and Chunlei, Z., "Denoising algorithm based on wavelet adaptive threshold." Physics Procedia, 24, pp.678-685. 2012., doi: https://doi.org/10.1016/j.phpro.2012.02.100

[32] M. Roy, V.R. Kumar, B.D. Kulkarni, J. Sanderson, M. Rhodes, and M.V. Stappen, 2000. "Simple denoising algorithm using wavelet transform." arXiv preprint nlin/0002028. doi: https://doi.org/10.48550/arXiv.nlin/0002028

[33] Bin Queyam, A., Kumar Pahuja, S. and Singh, D., "Quantification of feto-maternal heart rate from abdominal ECG signal using empirical mode decomposition for heart rate variability analysis." Technologies, 5(4), p.68. 2017, doi: https://doi.org/10.3390/technologies5040068

[34] S.D. Kreibig, " Autonomic nervous system activity in emotion: A review." Biol. Psychol. 2010, 84, 394–421.

[35] Y. Zhang, M. Haghdan, K.S. Xu, "Unsupervised motion artifact detection in wrist-measured electrodermal activity data." In Proceedings of the 2017 ACM International Symposium on Wearable Computers, Maui, HI, USA, 11–15 September 2017; pp. 54–57.

[36] S. S. Patil, M. K. Pawar, "Quality advancement of EEG by wavelet denoising for biomedical analysis." Proceedings - 2012 International Conference on Communication,Information and Computing Technology, ICCICT 2012, 1–6. doi: https://doi.org/10.1109/ICCICT.2012.6398151

[37] C.R. Harris, K.J. Millman, S.J. Van DerWalt, R. Gommers, P. Virtanen, D. Cournapeau, E. Wieser, J. Taylor, S. Berg, N.J. Smith, et al. Array programming with NumPy. Nature 2020, 585, 357–362.

[38] Emran Mohammad Abu Anas, Soo Yeol Lee, and Md Kamrul Hasan." Exploiting correlation of ecg with certain emd functions for discrimination of ventricular brillation." Computers in biology and medicine, 41(2):110-114, 2011.

[39] N. Ibtehaz, M.S. Rahman, " VFPred: a fusion of signal processing and machine learning techniques in detecting ventricular fibrillation from ECG signals". Biomedical Signal Processing and Control, 49, pp.349-359. doi: https://doi.org/10.1016/j.bspc.2018.12.016

[40] Long, L., Wen, X. and Lin, Y., 2021. Denoising of seismic signals based on empirical mode decomposition-wavelet thresholding. Journal of Vibration and Control, 27(3-4), pp.311-322.doi:https://doi.org/10.1177/1077546320926846